



THE UNIVERSITY *of* EDINBURGH

## Edinburgh Research Explorer

# The effect of pressure on the crystal structure of [Gd(PhCOO)(3)(DMF)](n) to 3.7 GPa and the transition to a second phase at 5.0 GPa

### Citation for published version:

Parois, P, Moggach, SA, Lennie, AR, Warren, JE, Brechin, EK, Murrie, M & Parsons, S 2010, 'The effect of pressure on the crystal structure of [Gd(PhCOO)(3)(DMF)](n) to 3.7 GPa and the transition to a second phase at 5.0 GPa' Dalton Transactions, vol. 39, no. 30, pp. 7004-7011. DOI: 10.1039/c0dt00046a

### Digital Object Identifier (DOI):

[10.1039/c0dt00046a](https://doi.org/10.1039/c0dt00046a)

### Link:

[Link to publication record in Edinburgh Research Explorer](#)

### Document Version:

Peer reviewed version

### Published In:

Dalton Transactions

### Publisher Rights Statement:

Copyright © 2010 by the Royal Society of Chemistry. All rights reserved.

### General rights

Copyright for the publications made accessible via the Edinburgh Research Explorer is retained by the author(s) and / or other copyright owners and it is a condition of accessing these publications that users recognise and abide by the legal requirements associated with these rights.

### Take down policy

The University of Edinburgh has made every reasonable effort to ensure that Edinburgh Research Explorer content complies with UK legislation. If you believe that the public display of this file breaches copyright please contact [openaccess@ed.ac.uk](mailto:openaccess@ed.ac.uk) providing details, and we will remove access to the work immediately and investigate your claim.



Post-print of a peer-reviewed article published by the Royal Society of Chemistry.

Published article available at: <http://dx.doi.org/10.1039/C0DT00046A>

Cite as:

Parois, P., Moggach, S. A., Lennie, A. R., Warren, J. E., Brechin, E. K., Murrie, M., & Parsons, S. (2010). The effect of pressure on the crystal structure of  $[\text{Gd}(\text{PhCOO})_3(\text{DMF})]_n$  to 3.7 GPa and the transition to a second phase at 5.0 GPa. *Dalton Transactions*, 39(30), 7004-7011.

Manuscript received: 28/02/2010; Accepted: 10/05/2010; Article published: 23/06/2010

# The effect of pressure on the crystal structure of $[\text{Gd}(\text{PhCOO})_3(\text{DMF})]_n$ to 3.7 GPa and the transition to a second phase at 5.0 GPa<sup>\*\*†</sup>

Pascal Parois,<sup>1</sup> Stephen A. Moggach,<sup>2</sup> Alistair R. Lennie,<sup>3</sup> John E. Warren,<sup>3</sup> Euan K. Brechin,<sup>2</sup> Mark Murrie,<sup>1,\*</sup> and Simon Parsons.<sup>2,\*</sup>

<sup>[1]</sup>WestCHEM, Department of Chemistry, University of Glasgow, University Avenue, Glasgow, UK.

<sup>[2]</sup>School of Chemistry and Centre for Science at Extreme Conditions, The University of Edinburgh, King's Buildings, West Mains Road, Scotland, UK.

<sup>[3]</sup>CCLRC Daresbury Laboratory, Warrington, Cheshire, UK.

<sup>[\*]</sup>Corresponding authors; M.M. e-mail: [M.Murrie@chem.gla.ac.uk](mailto:M.Murrie@chem.gla.ac.uk), S.P. e-mail: [S.Parsons@ed.ac.uk](mailto:S.Parsons@ed.ac.uk)

<sup>[\*\*]</sup>We thank the EPSRC for funding and the STFC for provision of synchrotron beam time.

<sup>[†]</sup>Dedicated to Professor David W. H. Rankin on the occasion of his retirement.

## Supporting information:

Electronic supplementary information (ESI) available: Table S1 and a movie showing the path of compression. CCDC reference numbers 768036–768039, 768040–768044. For ESI and crystallographic data in CIF or other electronic format see <http://dx.doi.org/10.1039/C0DT00046A>

## Graphical abstract:



## Synopsis:

As pressure is increased to 3.7 GPa (37 000 atm) on the polymer  $[\text{Gd}(\text{PhCOO})_3(\text{DMF})]_n$  the Gd...Gd distances compress by almost 0.2 Å. Short H...H contacts also develop between the complexes. On increasing the pressure to 5 GPa the structure undergoes a phase transition. An edge-edge phenyl-phenyl interaction is converted to a  $\pi$ ... $\pi$  stacking contact, relieving some of the short H...H contacts. The Gd...Gd distances increase in order to facilitate more efficient packing of the polymeric chains.

## Abstract

The effect of pressure on the crystal structure of the coordination polymer  $[\text{Gd}(\text{PhCOO})_3(\text{DMF})]_n$  has been studied to 5.0 GPa. At ambient pressure the structure is tetragonal (space group  $P4_2/n$ ) with the polymers extending along the  $c$ -direction of the unit cell; successive Gd atoms are alternately bridged by four benzoates and by two benzoates; the coordination spheres of the metal atoms are completed by DMF ligands. This results in two different Gd...Gd repeats, measuring 3.8953(3) and 5.3062(3) Å, respectively. The polymer chains interact with each other via dispersion interactions, including a number of CH... $\pi$  contacts to phenyl rings in which the H...ring-centroid distances are 3.19 to 3.28 Å. Up to 3.7 GPa the crystal remains in a compressed form of its ambient-pressure phase. The  $a$ -axis shortens by 7.7%, and the  $c$ -axis by 2.9%, the difference reflecting the greater ease of compression along the crystallographic directions mediated by weak intermolecular interactions. At ambient pressure the Gd-O distances span 2.290(2) – 2.559(2) Å, with an average of 2.39(3) Å. At 3.7 GPa the corresponding parameters are 2.259(3) to 2.509(4) and 2.36(3) Å. The Gd...Gd distances shortened by 0.0467(4) and 0.1851(4) Å, and the CH... $\pi$  distances span the range 2.76 – 2.90 Å. During compression a number of H...H contacts develop, the shortest measuring 1.84 Å at 3.7 GPa. On increasing the pressure to 5.0 GPa a phase transition occurred in which the shortest H...H contact is relieved by conversion of an edge-to-edge phenyl-phenyl contact into a  $\pi$ ... $\pi$  stacking interaction. The new phase is also tetragonal, space group  $P\bar{4}$ , the inversion symmetry present in phase-I being lost in phase-II. The phase transition allows more efficient packing of ligands, and while the  $a$ -axis decreases in length the  $c$ -axis increases. This leads to Gd...Gd distances of 3.8373(4) and 5.3694(4) Å, the latter being longer than at ambient pressure. Gd-O distances at 5.0 GPa span the range 2.265(5) to 2.516(5) Å, with a mean of 2.36(2) Å.

## Introduction

While high-pressure crystal structures of molecular compounds are not exactly common, there has been a distinct increase in the number of systems studied over the past 10 years. A search of the Cambridge Database<sup>1,2</sup> for entries containing the field *pressure* identified 135 individual compounds for which structural data are available above 0.1 GPa (1 kbar),<sup>‡</sup> 98 of which have been published since 2000. The majority of these compounds are organic, and only 14 contain a metal. With two exceptions (benzene and carbon dioxide) all data lie in the pressure range 0 – 10 GPa.

Broadly speaking, high-pressure single-crystal diffraction studies on metal complexes have been performed either to explore the compressibility of inter- and intra- molecular interactions or to explain the alterations of physical (especially magnetic) properties that occur at high pressure.<sup>3</sup> In the former category, the systems *cis*- $[\text{PdCl}_2([\text{9}]\text{aneS}_3)]$  (CSD refcode GATLES)<sup>4</sup> and  $[\text{GuH}][\text{Cu}_2(\text{OH})(\text{cit})(\text{Gu})_2]$  ( $\text{H}_4\text{cit}$  = citric acid,  $\text{Gu}$  =

<sup>‡</sup> The unit of pressure used here is the gigapascal (GPa). 1 atm =  $1.01325 \times 10^{-4}$  GPa. 1 GPa = 10 kbar ~ 10 000 atm. Pressures at the bottom of deep sea trenches reach around 1000 atm ~ 1 kbar = 0.1 GPa.

guanidine and GuH = guanidinium cation),<sup>5</sup> have been shown to undergo phase transitions at 4.6 GPa, in the case of the Pd complex, and at 2.9 and 4.2 GPa for the Cu complex, in which long intermolecular contacts involving the metal atoms have been transformed into primary coordination bonds. Compression of intermolecular interactions such as H-bonds and van der Waals contacts were explored in [Ru<sub>3</sub>(CO)<sub>12</sub>] (FOKNEY) to 8 GPa,<sup>6</sup> [Co<sub>2</sub>(CO)<sub>6</sub>(PPh<sub>3</sub>)] (CEDBUJ) to 4.6 GPa<sup>7, 8</sup> and [4-chloropyridinium][CoX<sub>4</sub>] (X= Cl, Br) (SAZZID) to 4 GPa.<sup>9</sup>

By-and-large, work on organic compounds has aimed to produce new high-pressure phases by rearrangement of intermolecular interactions. Although intramolecular conformational changes have also been observed in some of these studies, bond angles and distances are not greatly affected. For example, in serine hydrate some CC and CO bonds shortened by around 0.01 Å between ambient pressure and 3.8 GPa.<sup>10</sup> The same is not true in coordination compounds, where metal geometry is more flexible: changes in bond distances can be an order of magnitude greater than those seen in serine hydrate. In the work described above on *cis*-[PdCl<sub>2</sub>([9]aneS<sub>3</sub>)], for example, a Pd...S distance changed by 0.31 Å between ambient pressure and 4.25 GPa.<sup>4</sup>

The ability to affect intramolecular interactions has prompted a number of groups to explore the ability of pressure to tune physical properties governed by metal-metal or metal-ligand distances or the geometry around bridging groups. In the field of magnetism this work has shown that pressure is a very powerful means for studying magneto-structural correlations. For example, in [NMe<sub>4</sub>][MnCl<sub>3</sub>] (TMAMMN) parallel structural and magnetic measurements revealed an approximate  $r^{-10}$  dependence of the coupling constant with Mn...Mn distance ( $r$ ) pointing to the importance of direct exchange coupling between the metals.<sup>11</sup>

Single-molecule magnets (SMMs) have also been studied in this context,<sup>12-15</sup> and, outside of proteins, these are the most complex systems to have been investigated using high-pressure crystallography. Magnetic coupling in SMMs is mediated via super-exchange and therefore depends on the geometry of bridging ligands. The torsional flexibility of bridging (derivatised) salicylaldoxime (R-saoH<sub>2</sub>) ligands in [Mn<sub>6</sub>O<sub>2</sub>(Et-sao)<sub>6</sub>(O<sub>2</sub>CPh(Me)<sub>2</sub>)(EtOH)<sub>6</sub>] has enabled pressure to be used to reduce the magnitude of Mn-O-N-Mn torsion angles.<sup>13, 14</sup> This changes the interaction between pairs of Mn atoms from ferromagnetic to antiferromagnetic, leading to a reduction in the spin ground state for the complex and a lowering of the energy barrier for the reorientation of its magnetic moment. In the Mn<sub>12</sub>-acetate family of SMMs the existence of fast- and slow-relaxing species has been ascribed to the presence of Jahn-Teller isomers which differ in the orientation of the Jahn-Teller axis of a Mn(III) centre. A recent study on the complex [Mn<sub>12</sub>O<sub>12</sub>(O<sub>2</sub>CCH<sub>2</sub><sup>t</sup>Bu)<sub>16</sub>(H<sub>2</sub>O)<sub>4</sub>]·CH<sub>2</sub>Cl<sub>2</sub>·MeNO<sub>2</sub> showed that these isomers can be inter-converted using pressure, with parallel magnetic measurements showing corresponding conversion between fast and slow relaxation of the magnetisation.<sup>12</sup>

High pressure has also been used to study spin-crossover complexes of Fe(II). Ambient pressure and temperature usually favour the high-spin state; this has a higher volume than the low-spin state owing to occupation of antibonding e<sub>g</sub> orbitals, and as pressure increases the need to minimise the  $pV$  contribution to

free energy favours the lower volume low-spin state. Pressure-induced high-to-low spin transitions have been observed by single crystal diffraction in  $[\text{Fe}(\text{phen})_2(\text{NCS})_2]$  (KEKVIF) and  $[\text{Fe}(\text{Btz})_2(\text{NCS})_2]$  (PASGOF), where phen = 1,10-phenanthroline and Btz = 2,2'-bi-4,5-dihydrothiazine, at 1 and 0.5 GPa, respectively.<sup>16</sup> Other transitions have been followed by changes in cell dimensions tracked using powder diffraction.<sup>17</sup>

The ability to compress intra- and inter-molecular interactions has also excited interest in the field of metal-organic framework materials, where pressure has the potential to control uptake of different guests. This has recently been described in a study in which the unit cell volume of the zeolitic imidazole framework ZIF-8 was shown to *increase* under pressure as solvent molecules were forced into the pores, leading eventually to a new phase with enlarged channels at 1.47 GPa.<sup>18</sup>

High pressure is a valuable tool for controlling the properties of metal complexes, and when combined with crystallography the structural cause for the changes in properties is revealed. In all of the work described above the compounds studied were transition metal complexes, and no work has been reported on characterising the effect of pressure on the crystal structures of f-block complexes.

Our interest in lanthanide coordination chemistry stems from the potential of lanthanide ions as components of molecular magnetic materials. However, f-electrons interact weakly with surrounding ligands, so that exchange coupling between metal centres is weak. Compressing metal-ligand and metal-metal distances with pressure is a potential strategy for increasing magnetic exchange and in this paper we describe a high-pressure study on the one-dimensional coordination polymer  $[\text{Gd}(\text{PhCOO})_3(\text{DMF})]_n$  (**1**)

The crystal structure of **1** was first investigated by Lam *et al.*,<sup>19</sup> and is available on the Cambridge Database as refcode LUSCOR. One motive for selecting **1** was that it crystallises in a high symmetry space group ( $P4_2/n$ ). High-pressure single-crystal diffraction data sets are almost always incomplete because the pressure cell restricts the volume of the diffraction pattern that can be collected. This problem, which leads to a low data-to-parameter ratio during structure refinement, means that interatomic distances in high-pressure structures are less precise than in structures measured at ambient pressure. However, the problem is minimised if the diffraction pattern has high symmetry, and since we aim to measure Gd-O distances with a high enough precision for trends to be detected, high symmetry is a significant advantage.

A second feature of **1** which attracted our attention is that it is a one-dimensional polymer formed along a unit cell axis in a high-symmetry crystal system. In this case the polymer is formed along the *c*-direction of a tetragonal unit cell. These factors mean that, to a first order of approximation, the intramolecular interactions are directed along one direction (*c*), with the weaker van der Waals interactions forming in the other directions (*a* and *b*). The tetragonal symmetry of the structure means that the principal axes of strain lie along the unit cell axes, so that simple comparison of the changes in the *a* and *c* unit cell lengths is a measure of the relative compressibility of the intra- and inter- molecular bonds. In addition, the Gd...Gd vectors lie along one of the principal strain directions.

The present study therefore enables us to address two questions: (i) to what extent can intramolecular lanthanide-ligand and lanthanide-lanthanide distances be changed with pressure? and (ii) how compressible are intramolecular bonds in lanthanide complexes relative to intermolecular contacts between organic ligands?

## Experimental

### *Synthesis and crystal growth of 1<sup>19</sup>*

Benzoic acid (6 mmol) and NaOH (6 mmol) in methanol (15 mL) were stirred at room temperature for 30 min and a solution of Gd(NO<sub>3</sub>)<sub>3</sub>·6H<sub>2</sub>O (2 mmol) in methanol (5 mL) was added. After 4 hours stirring at ambient temperature, the white precipitate was filtered and washed with methanol. The product was dissolved in hot dimethylformamide (DMF); colourless single crystals of [Gd(PhCOO)<sub>3</sub>(DMF)]<sub>n</sub> (**1**) were obtained after 3 days.

### *High Pressure Crystallography: General Procedures*

High-pressure experiments were carried out with a modified Merrill-Bassett diamond anvil cell (DAC) equipped with 600 μm culet diamonds and a tungsten gasket.<sup>20, 21</sup> The sample and a chip of ruby (as a pressure calibrant) were loaded into the DAC with a 4:1 mixture of methanol and ethanol as a hydrostatic medium. The ruby fluorescence method was utilised to measure the pressure.<sup>22</sup>

### *Data Collection, Reduction and Refinement*

A sphere of data was collected on a crystal of **1** at ambient temperature and pressure in order to provide data for comparison with the high-pressure studies, which were also performed at ambient temperature (see below). Diffraction data were collected on a single crystal on a Bruker SMART APEX diffractometer with graphite-monochromated Mo-Kα radiation ( $\lambda = 0.71073 \text{ \AA}$ ). These data were integrated using the program SAINT,<sup>23</sup> and the absorption correction was carried out using the program SADABS.<sup>24</sup> Refinement was carried out against  $|F|^2$  using all data (CRYSTALS)<sup>25</sup> starting from the ambient temperature coordinates of ref.<sup>19</sup>. We show below that **1** undergoes a phase transition at high pressure, and the usual origin choice of the space group of the low-pressure phase was moved from the centre of inversion to the  $\bar{4}$  site (origin choice 1 in International Tables), in order to facilitate comparison of the two phases. The final conventional *R* factor was 0.024 for 7016 data.

High-pressure diffraction data were collected with synchrotron radiation on a Bruker APEX II diffractometer at the STFC Daresbury Laboratory on Station 9.8 ( $\lambda = 0.4865 \text{ \AA}$ ). Data were collected in  $\omega$ -scans in eight settings of  $2\theta$  and  $\phi$  with a frame and step size of one second and  $0.3^\circ$ , respectively. This data collection

strategy was based on that described in ref. <sup>26</sup>. The data were integrated using the program SAINT using 'dynamic masks' to avoid integration of regions of the detector shaded by the body of the pressure cell.<sup>26</sup> Absorption corrections for the DAC and sample were carried out with the program SADABS. Data were collected at 0.10, 0.55, 1.18, 1.67, 2.65, 3.20, 3.73, 5.01 and 6.10 GPa.

Refinements starting from the published coordinates were carried out against  $|F|^2$  using all data (CRYSTALS).<sup>25</sup> The structure at 5.0 GPa was solved using direct methods (SIR92).<sup>27</sup> All 1,2 and 1,3 distances of the dimethylformamide and benzoate ligands were restrained to the values observed from our ambient pressure structure. All torsion angles and metal to ligand distances were refined freely. Hydrogen atoms attached to carbon were placed geometrically and not refined.

All C, N and O atoms were refined with isotropic thermal parameters to 5.0 GPa, while the Gd atoms were refined anisotropically. Above 5.0 GPa, the data quality deteriorated and no acceptable refinement could be obtained for the final 6.1 GPa data set. The cell dimensions at 6.1 GPa were  $a = 19.4090(4)$ ,  $c = 9.3837(3)$  Å,  $V = 3534.9(3)$  Å<sup>3</sup>. The deterioration of the data quality was the result of increasing mosaic spread with increasing pressure, a frequently encountered problem with crystallographic pressure studies on molecular materials. Listings of crystal and refinement data for the structures of **1** at ambient temperature and pressure are given in Table 1, data for other pressures are available in the supplementary material.

Phase	I	I	II
Pressure (GPa)	0 (ambient)	3.7	5.0
<i>Crystal data</i>			
Chemical formula	$(C_{24}H_{22}GdNO_7)_n$		
$M_r$	593.69		
Crystal system, space group	Tetragonal, $P4_2/n$	Tetragonal, $P4_2/n$	Tetragonal, $P-4$
$a, c$ (Å)	22.4915 (6), 9.1640 (3)	20.7490 (3), 8.8988 (2)	20.0734 (2), 9.1385 (1)
$V$ (Å <sup>3</sup> )	4635.8 (2)	3831.12 (12)	3682.28 (7)
$Z$	8	8	8
$\mu$ (mm <sup>-1</sup> )	2.91	1.12	1.17
Crystal size (mm)	0.23 × 0.16 × 0.12	0.20 × 0.20 × 0.10	0.20 × 0.20 × 0.10
<i>Data collection</i>			
$T_{min}, T_{max}$	0.56, 0.71	0.27, 0.70	0.34, 0.69
No. of measured, independent and observed [ $I > 2.0\sigma(I)$ ] reflections	77931, 7016, 4714	21264, 3398, 2646	19799, 6303, 5867
$d_{min}$ (Å)	0.7	0.7	0.7
Completeness	0.989	0.582	0.586
$R_{int}$	0.067	0.069	0.068
<i>Refinement</i>			
$R[F^2 > 2\sigma(F^2)], wR(F^2), S$	0.024, 0.068, 1.05	0.032, 0.037, 1.12	0.051, 0.054, 0.94
No. of reflections	7016	2646	5867
No. of parameters	298	298	275
No. of restraints	0	86	172
$\Delta\rho_{max}, \Delta\rho_{min}$ (e Å <sup>-3</sup> )	1.48, -1.18	0.80, -0.75	1.96, -2.62

**Table 1.** Crystal and refinement data for the structures of **1** at ambient pressure, 3.7 GPa and 5.0 GPa.

Crystal structures were visualized using the programs DIAMOND,<sup>28</sup> XP<sup>29</sup> and MERCURY.<sup>30</sup> A movie, available in the supplementary material, showing the path of compression was produced using CrystalMaker.<sup>31</sup> Geometric calculations were carried out using PLATON,<sup>32</sup> as incorporated in the WIN-GX suite.<sup>33</sup> Searches of the Cambridge Database<sup>1</sup> were performed with the program CONQUEST and version 5.31 of the database with updates up to November 2009.<sup>2</sup> The bulk modulus of **1** was calculated using EOSFIT.<sup>34-36</sup>

## Results and Discussion

### *The structure of [Gd(PhCOO)<sub>3</sub>(DMF)]<sub>n</sub> (**1**) at ambient pressure*

The unit cell of **1** consists of four 1D chains oriented along the *c*-direction, with the asymmetric unit consisting of one Gd(III), three benzoates and one DMF. The Gd(III) ions are coordinated by eight oxygen atoms in a distorted square antiprism arrangement. The metals are bridged by benzoate ligands in either 1,3 or 1,1',3-modes, with one DMF molecule completing each coordination sphere (see Fig. 1*i*). The polymer chain is generated by successive inversion centres and the distance between Gd centres alternates. The longer distance [Gd1...Gd1B, 5.3062(3) Å] corresponds to the distance between Gd centres bound between two symmetry equivalent 1,3-bridging benzoate ligands based on O5/O6 and two equivalent DMF ligands. The shorter Gd...Gd distance [Gd1...Gd1A, 3.8953(3) Å] is spanned by two 1,3-bridging and two 1,1',3-bridging benzoate ligands based on O3/O4 and O1/O2, respectively.

The longer Gd...Gd distance is spanned by a number of inter-ligand CH... $\pi$  interactions (Fig 1*ii*), notably to the phenyl ring based on C16-C21, which forms a CH... $\pi$  interaction on one face to H61 and on the other to H141. The dihedral angles between the phenyl rings involved in these interactions are 80.96(19)° and 55.48(19)°, respectively; the normalised H...centroid distances are 3.09 and 2.90 Å. A H- $\pi$  contact involving H243 derived from a DMF ligand and the centroid of the ring based on C2-C7 measures 3.23 Å.

The shortest atom-atom distances between the polymer chains also take the form of CH... $\pi$  interactions involving H-atoms derived from phenyl and methyl groups (shown in Fig. 2*i* as blue and cyan dashed lines). The normalised H...centroid distances in these interactions span the range 3.19 – 3.28 Å; the angle between the phenyl groups involved in the blue CH... $\pi$  contacts in the middle of the cell in Fig. 2*i* is 87°. These interactions are relatively long,<sup>37</sup> and the principal interaction is best considered as dispersion along the lengths of the polymer chains rather than in terms of specific atom-atom contacts.



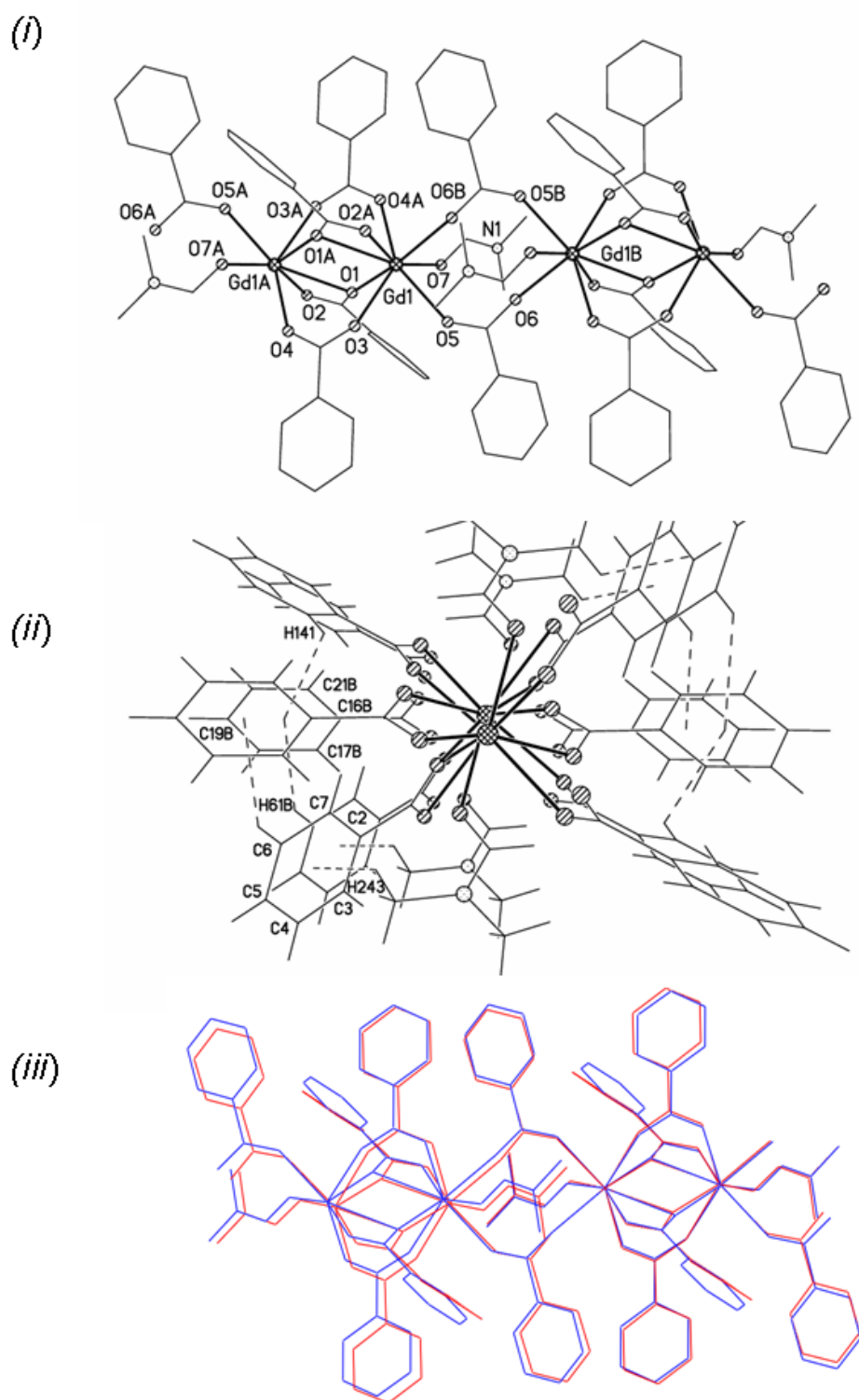


**Figure 1.** The structure of **1** in phase I. (i) View of the ambient-pressure structure perpendicular to the *c*-axis showing coordination of the Gd atoms and the two different Gd...Gd distances. (ii) View along the *c*-axis showing CH... $\pi$  contacts. (iii) Superposition of the polymer chains at ambient pressure (blue) and 3.7 GPa (red).

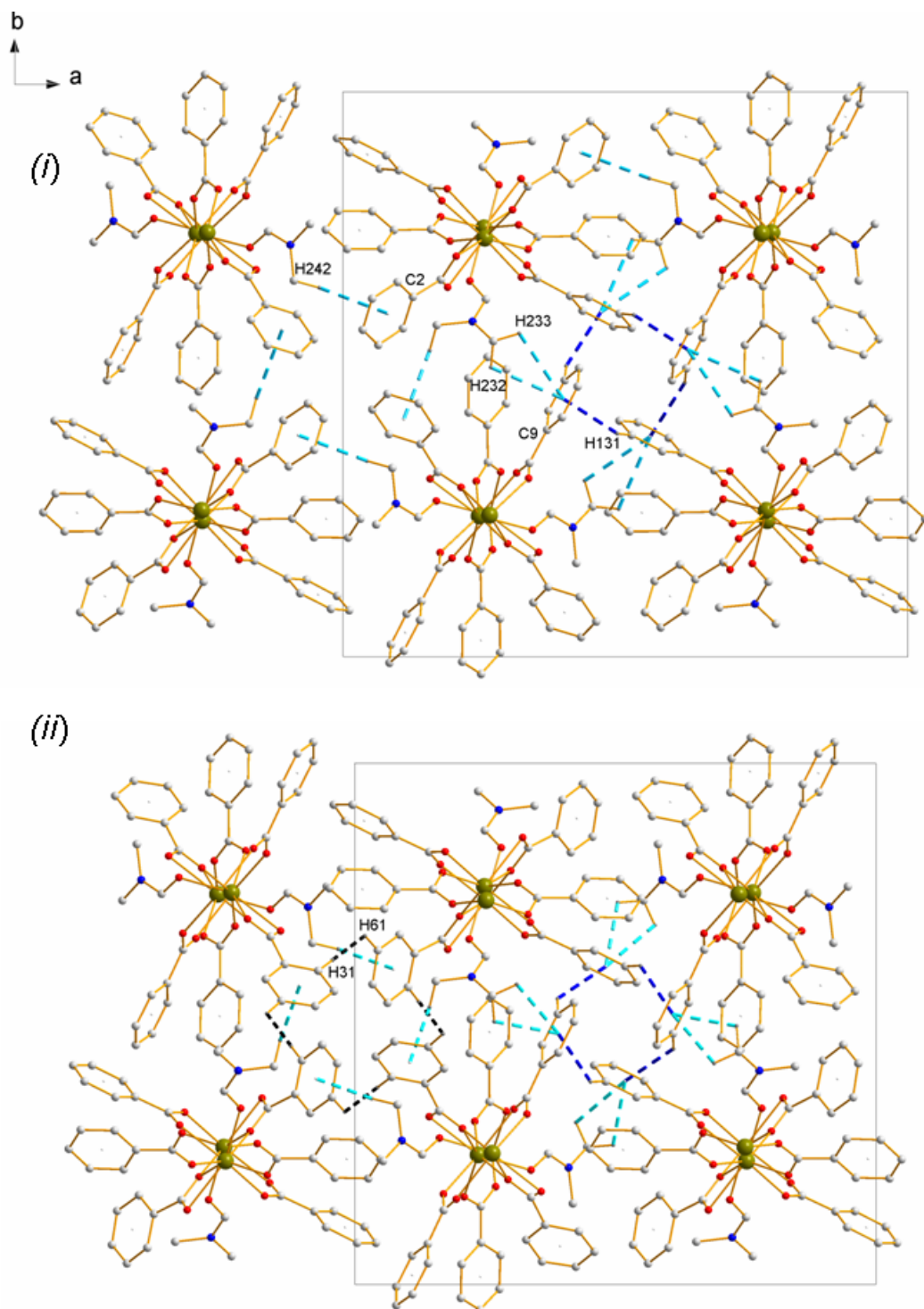


**Figure 2.** Packing in **1** as viewed along the *c*-axis at ambient pressure (*i*), 3.7 GPa (*ii*) and 5.0 GPa (*iii*). CH... $\pi$  contacts ( $< 3.3$  Å at ambient pressure and  $< 3$  Å at 3.7 and 5.0 GPa) involving methyl and phenyl hydrogen atoms are shown in cyan and blue, respectively. Short H...H contacts ( $< 2$  Å) are shown in black in (*ii*) and (*iii*). The  $\pi$ ... $\pi$  contact generated after the phase transition in (*iii*) is shown as a red dashed line about half way along the vertical (*b*) axis. Gd atoms are olive green, O atoms are red, N atoms are blue, H and C atoms are grey. All three figures are on the same scale, H-atoms not involved in contacts have been deleted for clarity.

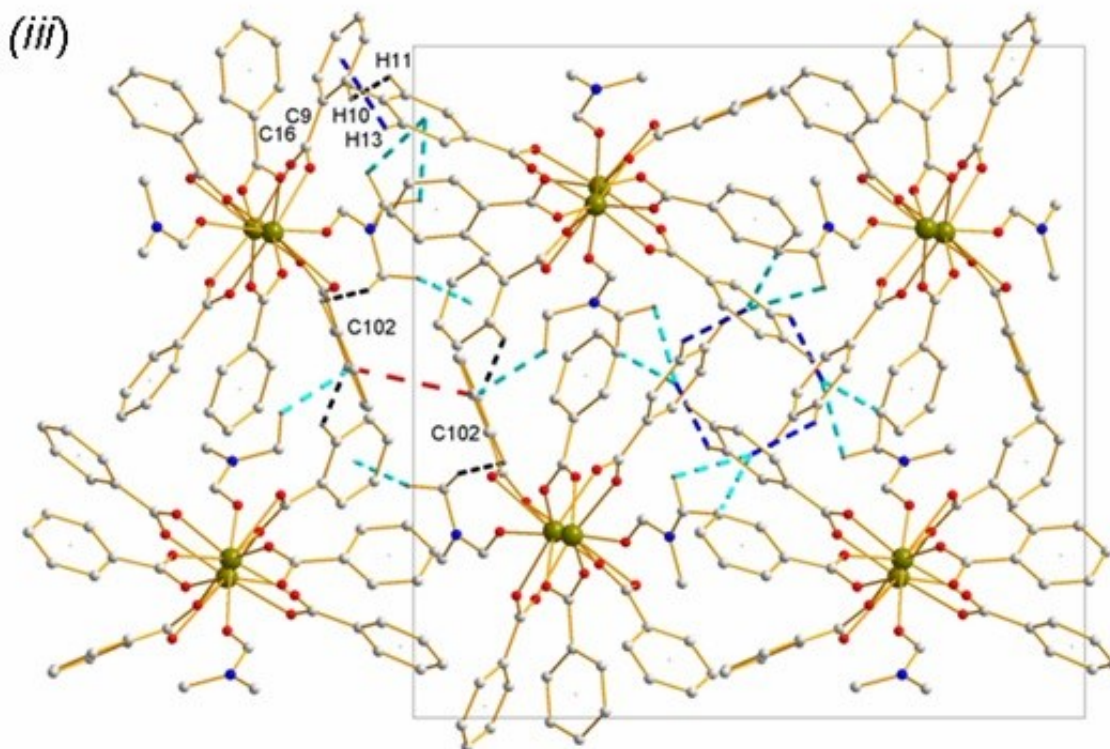


**Figure 2.** (continued)

On increasing pressure, the structure of **1** was found to be stable to 3.7 GPa. Above this pressure, the compound undergoes a single-crystal to single-crystal phase transition to a previously unknown high-pressure phase which we have designated **1-II**, referring to the previous phase as **1-I**.

#### *The compressibility of 1-I*

On increasing pressure to 3.7 GPa, the greatest compression in the structure occurs within the *ab*-face, with a 7.7% decrease in the length of the *a* and *b*-unit cell dimensions, while the *c*-axis reduces by only 2.9%. As a result of the tetragonal symmetry the principal axes of the strain tensor lie in the same directions.

Evolution of the cell parameters of **1-I** as a function of pressure are shown in Fig. 3. The bulk modulus,  $K_0$ , fitted to a Vinet equation of state<sup>38,39</sup> is 8.3(9) GPa and its pressure derivative ( $K'$ ) is 9.3(13). These data fall between those for  $\text{Ru}_3(\text{CO})_{12}$  ( $K_0 = 6.6$  GPa) and L-alanine [ $K_0 = 13.6(7)$  GPa,  $K' = 6.7(4)$ ].<sup>40</sup> The higher the bulk modulus the more resistant a solid is towards compression, and **1** is a relatively soft material. That the value should lie between those for a van der Waals solid such as  $\text{Ru}_3(\text{CO})_{12}$ <sup>6</sup> and a hydrogen bonded solid such as alanine seems intuitively reasonable. A more substantial decrease in the length of the *a* and *b*-unit cell dimensions over *c* is also unsurprising, as this results in a compression between the polymer chains, while any decrease in the length of the *c*-axis would result in a shortening of the chain along its backbone.

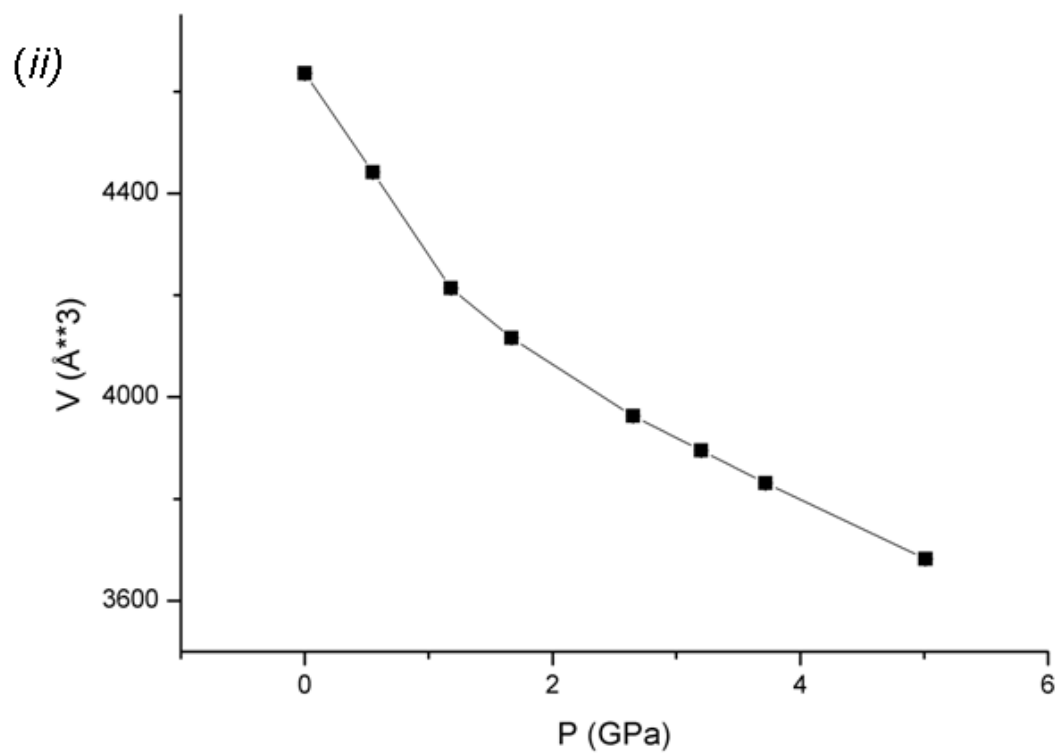
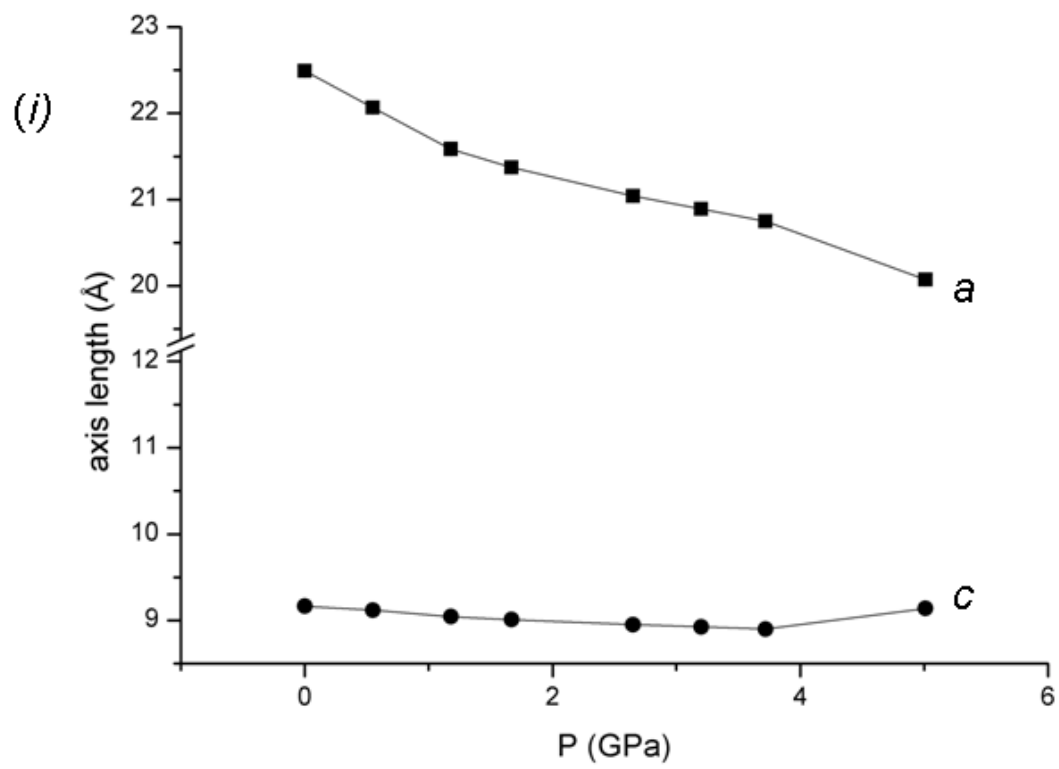


**Figure 3.** Variation of the cell axes (i) and volume (ii) with pressure.

### *Effect of pressure on the structure of 1-I up to 3.7 GPa*

Changes that occur to the structure between ambient pressure and 3.7 GPa can be conveniently visualised in the form of a movie shot along the *c*-direction of the unit cell. This is available in the supplementary information as file `gd_polymer_along_c.mov` (Quicktime format).

During refinement of the high-pressure structures all 1,2 and 1,3 distances on the benzoate and DMF ligands were restrained to their ambient pressure values. Torsion angles, which are more susceptible to pressure, were allowed to refine freely. Restraints were not applied to metal-ligand bond lengths as these can vary significantly with pressure.

Between ambient pressure and 3.7 GPa significant changes occur for all Gd-O bonds. At ambient pressure the range of Gd-O distances is 2.290(2) to 2.559(2) Å; at 3.7 GPa the corresponding data are 2.259(3) – 2.509(4) Å. The largest contraction [0.123(3) Å] occurs for Gd1-O1A bond (Fig 1*i*, Table 2). This bond, which is the longest Gd-O bond in the ambient pressure structure, is formed to the doubly bridging oxygen atom of the 1,1',3-bridging carboxylate. With the exception of Gd1-O2A and Gd1-O4A, which actually increase in length, the other Gd-O distances decrease by between 0.01 and 0.03 Å. At ambient pressure and 3.7 GPa the mean Gd-O distances are 2.39(3) Å and 2.36(3) Å, respectively.

Phase	I		II			
	0	3.7		5.0		5.0
Gd1-Gd1A	3.8953(3)	3.8486(3)	Gd1-Gd	3.8373(4)		
Gd1-Gd1B	5.3062(3)	5.1211(3)	Gd2-Gd1A	5.3694(4)		
Gd1-O1	2.3184(19)	2.298(3)	Gd1-O10	2.335(6)	Gd2-O1	2.292(5)
Gd1-O1A	2.559(2)	2.436(3)	Gd1-O1	2.516(5)	Gd2-O10	2.508(6)
Gd1-O2A	2.485(2)	2.509(4)	Gd1-O2	2.463(7)	Gd2-O20	2.502(7)
Gd1-O3	2.385(2)	2.367(3)	Gd1-O30	2.309(7)	Gd2-O3	2.444(7)
Gd1-O4A	2.360(2)	2.372(3)	Gd1-O4	2.285(6)	Gd2-O40	2.342(7)
Gd1-O5	2.3365(19)	2.307(3)	Gd1-O50	2.273(6)	Gd2-O5A	2.268(6)
Gd1-O6B	2.290(2)	2.259(3)	Gd1-O6	2.265(5)	Gd2-O60A	2.297(6)
Gd1-O7	2.402(2)	2.371(3)	Gd1-O70	2.356(7)	Gd2-O7	2.374(7)

**Table 2.** Gd-O bond distances (Å) in **1** as a function of pressure (in GPa). In phase I the symmetry operators corresponding to labels A and B are inversions  $-x+3/2, -y+3/2, -z-1/2$  and  $-x+3/2, -y+3/2, -z+1/2$ , respectively. In phase II the label A refers to the translation operator  $x, y, z+1$ . Angles are given in Table S1 in the supplementary material.

A search of the CSD database using a Gd(III) ion coordinated by eight O-atoms gives 95 hits excluding powder diffraction data, disordered structures and all structures with errors or an  $R$ -factor  $> 7.5\%$ . The frequency of Gd-O bonds as a function of distance drops off drastically below 2.26 Å; refcode FITJAU gives the smallest Gd-O distance, with 2.219(7) Å.<sup>41</sup> The minimum Gd-O distance in our complex at ambient pressure is Gd1-O6B [2.290(2) Å], which reduces to 2.259(3) Å at 3.7 GPa and remains the shortest Gd-O bond. These values therefore place Gd1-O6B towards the lower end of Gd(III)-O interactions seen at ambient pressure, but not outside it: there are no Gd-O bonds that would be considered abnormally short were they to be observed at ambient pressure.

Changes in bond angles are also significant (Table S1 in the supplementary material). The largest bond angle changes occur for Gd1-O5-C15 and Gd1-O6B-C15B, which decrease by 8.0(4) and 7.7(4)°, respectively. Other Gd-O-C angles vary by between 2.4 and 4.2°. The most prominent angular changes occur across the longer Gd...Gd distance; this correlates with the observation that between ambient pressure and 3.7 GPa the longer Gd...Gd distance contracts more than the shorter: 0.1851(4) versus 0.0467(4) Å, respectively.

Fig. 1iii is an overlay of the polymer structures at ambient pressure (blue) and 3.7 GPa (red) in which the coordination environments of one of the Gd atoms have been fitted. It is immediately apparent that the largest geometric changes occur for torsion angles. This is also true in organic structures, but here the magnitudes of the changes which occur are, by comparison, quite substantial given that at 3.7 GPa the structure is still in a compressed form of its ambient-pressure phase. The largest changes in torsion angles about the metal atoms appear to be associated with the largest changes in distances and angles described above. The Gd1-O1 contraction is accompanied by a twisting of the carboxylate group, with the Gd1-O1-C1-O2 torsion angle increasing from -137.1(4) to -152.4(5)°. The contraction of the longer Gd...Gd distance is accompanied by a change in the Gd1-O5-C15-O6 torsion angle through the carboxylate group from 35.3(5) to 40.1(6)°. The largest torsion angle change amongst the phenyl rings occurs for the ligand based on O1, where  $\tau(\text{O2-C1-C2-C3})$  increases from 23.9(4)° to 36.2(6)°.

The phenyl CH... $\pi$  contacts formed along the polymer (Fig. 1ii) from H141 and H61 shorten to 2.40 and 2.63 Å; the aliphatic CH... $\pi$  interaction from H241 shortens to 2.76 Å. The normalised CH... $\pi$  intermolecular distances described above decrease to a range of 2.76 to 2.90 Å (Fig. 2ii). In addition, a number of short H...H contacts develop (1.84 to 2.05 Å, shown in black in Fig. 2ii). The shortest contact is formed between H31 and H61. A survey of H...H contacts in high-pressure ( $< 10$  GPa) crystal structures by Wood *et. al.* found that normalised H...H distances do not compress below 1.7 Å and that the frequency of H...H contacts as a function of distance drops off drastically between 1.9 Å and 1.7 Å.<sup>42</sup> It is notable that the short contact between H31 and H61 increases as a result of the phase transition above 3.7 GPa, and it is possible that the transition is driven in part by relief of this interaction.

### The structure of I–II at 5.0 GPa

Between 3.7 and 5.0 GPa the crystal undergoes a single-crystal to single-crystal phase transition from  $P4_2/n$  to  $P\bar{4}$ , forming I-II. The symmetry change involves loss of inversion (along with glide and screw-axis) symmetry, but since the cell contents do not change, the size of the asymmetric unit doubles. The cell parameter  $a$  decreases from 20.7490(3) Å to 20.0734(2) Å and the cell volume from 3831.12(12) Å<sup>3</sup> to 3682.28(7) Å<sup>3</sup>. However, the  $c$ -axis increases from 8.8988(2) Å to 9.1385(1) Å. The increase in the  $c$ -axis and the packing modification allows a better interpenetration of the chains and thus allows a higher packing density (Fig. 2ii).

The overall structure of the polymer chain is unchanged through the transition and ligands retain their coordination motifs (Fig. 4i) with CH... $\pi$  interactions formed along the polymer chain (Fig. 4ii). An overlay of the polymer chains in phases I and II is shown in Fig. 4iii.

Bond distances and angles in phases I and II are correlated in Table 2. The ranges of Gd-O distances are rather similar in phase-I at 3.7 GPa [2.259(3) – 2.509(4) Å] and phase-II at 5.0 GPa [2.265(5) – 2.516(5) Å]. As the transition proceeds some bonds become longer (e.g. Gd1-O1A), some become shorter (e.g. Gd1-O4), while others become longer at one Gd atom and shorter at the other (e.g. Gd1-O3). The Gd-O bond (Gd1-O1A) which had suffered the largest shortening as phase-I was compressed becomes almost as long as it was at ambient pressure (2.436(3) Å at 3.7 GPa  $\rightarrow$  2.516(5) and 2.508(6) Å at 5.0 GPa). The shortest bond at 3.7 GPa (Gd1-O6B) increases from 2.259(3) Å in phase-I to 2.265(5) and 2.297(6) Å in phase-II. The mean Gd-O distance is 2.36(2) Å, that is, very similar to the mean Gd-O distance at 3.7 GPa. Likewise, increases and decreases are seen for O-Gd-O bond angles (Table S1). The largest increase [14.1(2)°] occurs as the O2A-Gd1-O3 transforms into O3-Gd2-O20 in phase-II. The largest decrease [-11.4(2)°] occurs for O2A-Gd1-O7  $\rightarrow$  O2-Gd1-O70.

The shorter Gd...Gd distance shortens slightly [0.0113(5) Å] between 3.7 and 5.0 GPa, while the longer increases substantially [0.2483(5) Å], reflecting the increase in the length of the  $c$ -axis. The longer Gd...Gd distance is, in fact, longer than it was at ambient pressure.

Fig. 4iii shows that conformational changes occur both at the metals and in the orientations of the phenyl rings. Loss of inversion symmetry means that torsion angles that were equal in magnitude but opposite in sign now have unrelated values. With respect to the phenyl ring orientations, the largest difference occurs for O2A-C1A-C2A-C3A, which changes from -36.2(6) to 14.4(12)°. This conformational change breaks the CH<sub>methyl</sub>... $\pi$  contacts that were formed along the polymer chain in phase-I (cf Figs. 1ii and 4ii). The CH<sub>phenyl</sub>... $\pi$  contacts now span the range 2.32–2.57 Å.

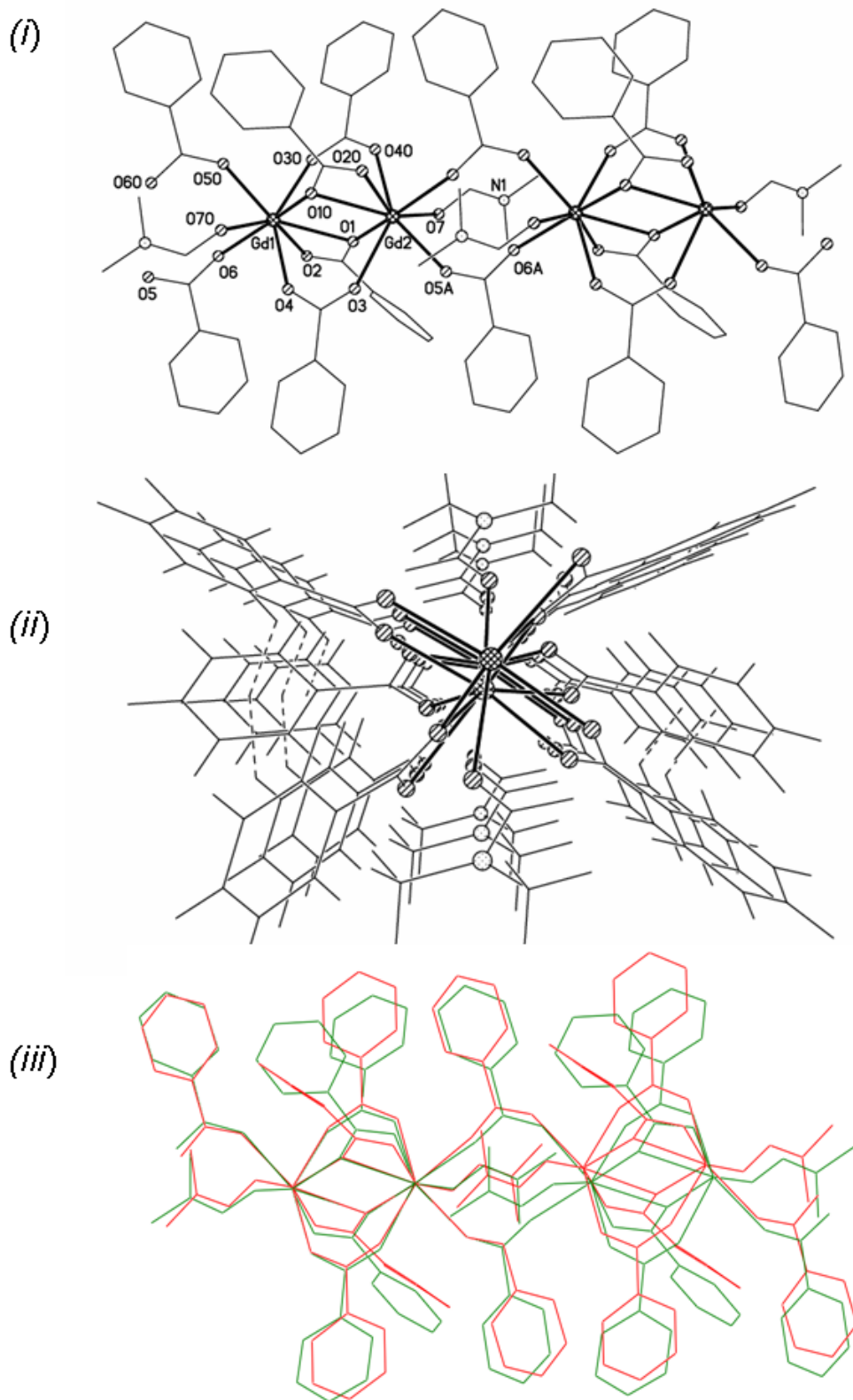


**Figure 4.** The structure of **1** in phase II at 5.0 GPa. (i) View of the structure perpendicular to the *c*-axis showing coordination of the Gd atoms, of which there are now two in the asymmetric unit. (ii) View along the *c*-axis showing CH... $\pi$  contacts. Notice that in contrast to phase-I the H-atoms all originate from phenyl groups. (iii) Superposition of the polymer chains at 3.7 GPa (red) and 5.0 GPa (green).



The changes in the phenyl ring orientations also affect the intermolecular packing, and an edge-to-edge interaction involving a pair of symmetry-related phenyl rings based on C102 is converted into an offset  $\pi$ - $\pi$  stacking interaction (the new interaction is shown as a red dotted line in Fig. 2iii). This rearrangement relieves the short H...H contact shown in Fig 2ii. The new stacking interaction is characterised by a centroid-centroid distance of 3.779(4) Å and an interplanar angle of 5°. The perpendicular distance between one centroid and its projection on the opposite ring is 3.105(3) Å and the offset between the two centroids when projected onto the same plane is 2.154(5) Å. Perpendicular stacking and off-set distances in other  $\pi$ ... $\pi$  interactions identified in a search of the CSD are depicted in Fig. 5. The search criteria used are described in the figure caption. The point corresponding to the offset and stacking distances in 1-II is also indicated on Fig. 5, and it is clear that this combination is rather uncommon. It is presumably stabilised by the high pressure.

Other contacts take the form of CH... $\pi$  contacts which follow much the same pattern as in phase-I. Though the conformational change described in the previous paragraph relieves the short H...H contact shown in Fig 2ii, several other H...H contacts are present at 5.0 GPa between 1.89 and 2.00 Å, and these are shown as black dotted lines in Fig. 2iii

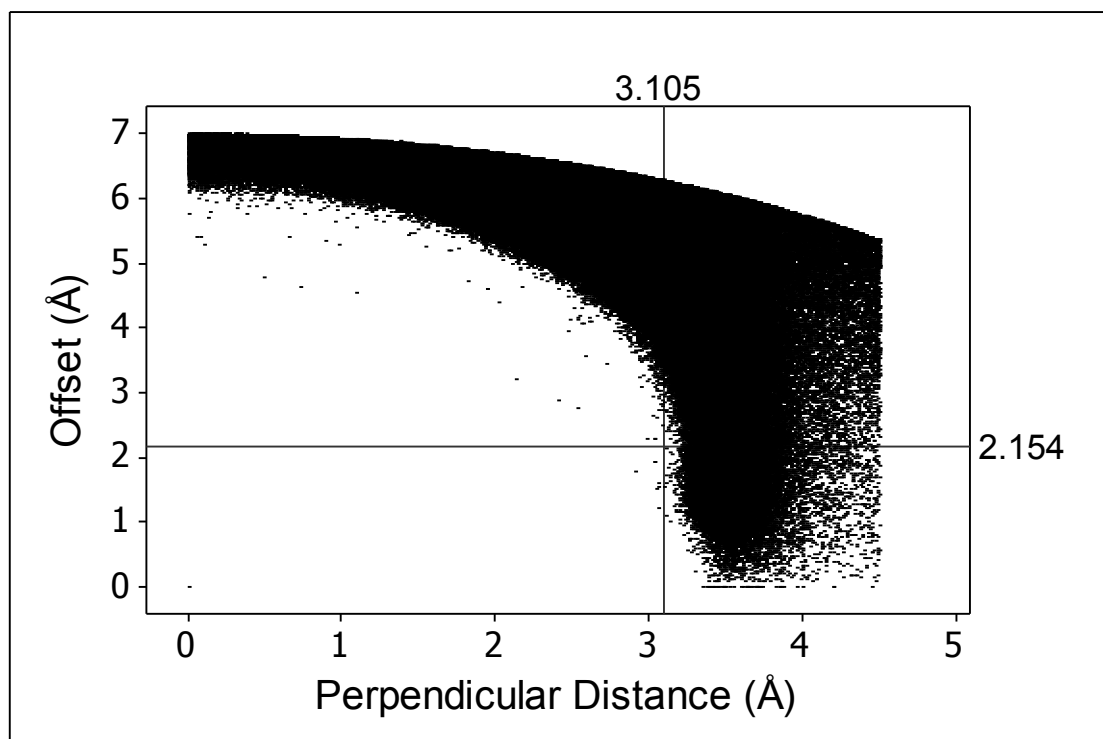


**Figure 5.** The geometry of stacked phenyl-phenyl interactions in the Cambridge Database. The parameters plotted are the perpendicular distance between one centroid and its projection on the opposite ring, and the offset between the two centroids when projected onto the same plane. The cross-hairs mark the position of the stacked interaction established in phase-II after the phase transition. The following parameters defined the search: the angle between the two planes formed by the phenyl groups lies between 0° and 10°; the distance

between the centroid of a phenyl group to the plane defined by the second phenyl group lies between 0 and 4.5 Å; the distance between two centroids lies between 0 and 7 Å. The offset distance can be calculated from the two previous distances by Pythagoras' Theorem. Structures with disorder, errors, data from powder diffraction and structures with an *R*-factor above 5% were not included. The total number of hits was 89661.

## Conclusions

We have described the effect of pressure on the crystal structure of the lanthanide-containing coordination polymer [Gd(PhCOO)<sub>3</sub>(DMF)]<sub>n</sub> (**1**). Up to 3.7 GPa the crystal structure remains in a compressed form of its ambient pressure phase. The structure packs so that the covalent polymer chains are orientated along the *c*-axis of the unit cell, with weaker van der Waals (notably CH... $\pi$ ) interactions between them directed in the *ab* plane. Accordingly, up to 3.7 GPa the unit cell compresses almost three times more in the *a*- and *b*-directions than in the *c*-direction.

At 3.7 GPa some very short H...H contacts are present and when the pressure was raised to 5.0 GPa the structure underwent a phase transition, where these short contacts were relieved by conversion of an edge-to-edge phenyl-phenyl contact into  $\pi$ ... $\pi$  interactions, though these have a rather unusual geometry compared to other such interactions in the Cambridge Database. Over the course of the transformation the *a*- and *b*-axes decrease in length, but the *c*-axis increases, pointing to more efficient interleaving of the ligands on neighbouring polymer chains.

Gd-O distances vary by as much as 0.12 Å, which is a larger value than is observed in purely organic structures over a similar range of pressure. However, they do not stray beyond the range of distances observed for similar bonds at ambient pressure. There is thus no structural evidence that there is any change in the bonding of the f-electrons. Much more strongly affected are the Gd...Gd distances, some of which at 3.7 GPa have shortened by almost 0.2 Å.

## References

- [1] F. H. Allen, *Acta Cryst.*, 2002, **B58**, 380-388.
- [2] F. H. Allen and W. D. S. Motherwell, *Acta Cryst.*, 2002, **B58**, 407-422.
- [3] S. A. Moggach and S. Parsons, *Spectrosc. Prop. Inorg. Organomet. Compd.*, 2009, **40**, 324-354.
- [4] D. R. Allan, A. J. Blake, D. Huang, T. J. Prior and M. Schroeder, *Chem. Comm.*, 2006, 4081-4083.
- [5] S. A. Moggach, K. W. Galloway, A. R. Lennie, P. Parois, N. Rowantree, E. K. Brechin, J. E. Warren, M. Murrie and S. Parsons, *CrystEngComm*, 2009, **11**, 2601-2604.
- [6] C. Slebodnick, J. Zhao, R. Angel, B. E. Hanson, Y. Song, Z. Liu and R. J. Hemley, *Inorg. Chem.*, 2004, **43**, 5245-5252.
- [7] N. Casati, P. Macchi and A. Sironi, *Angew. Chem., Int. Ed. Engl.*, 2005, **44**, 7736-7739.
- [8] N. Casati, P. Macchi and A. Sironi, *Chem.--Eur. J.*, 2009, **15**, 4446-4457.
- [9] G. M. Espallargas, L. Brammer, D. R. Allan, C. R. Pulham, N. Robertson and J. E. Warren, *J. Am. Chem. Soc.*, 2008, **130**, 9058-9071.
- [10] R. D. L. Johnstone, D. Francis, A. R. Lennie, W. G. Marshall, S. A. Moggach, S. Parsons, E. Pidcock and J. E. Warren, *CrystEngComm*, 2008, **10**, 1758-1769.
- [11] S. Tancharakorn, F. P. A. Fabbiani, D. R. Allan, K. V. Kamenev and N. Robertson, *J. Am. Chem. Soc.*, 2006, **128**, 9205-9210.
- [12] P. Parois, S. A. Moggach, J. Sanchez-Benitez, K. V. Kamenev, A. R. Lennie, J. E. Warren, E. K. Brechin, S. Parsons and M. Murrie, *Chem. Comm.*, 2010, DOI: 10.1039/B923962F.
- [13] A. Prescimone, C. J. Milios, S. A. Moggach, J. E. Warren, A. R. Lennie, J. Sanchez-Benitez, K. Kamenev, R. Bircher, M. Murrie, S. Parsons and E. K. Brechin, *Angew Chem Int Ed Engl* 2008, **47**, 2828-2831.
- [14] A. Prescimone, C. J. Milios, J. Sanchez-Benitez, K. V. Kamenev, C. Loose, J. Kortus, S. Moggach, M. Murrie, J. E. Warren, A. R. Lennie, S. Parsons and E. K. Brechin, *Dalton Trans.*, 2009, 4858-4867.
- [15] A. Prescimone, J. Sanchez-Benitez, K. V. Kamenev, S. A. Moggach, A. R. Lennie, J. E. Warren, M. Murrie, S. Parsons and E. K. Brechin, *Dalton Trans.*, 2009, 7390-7395.
- [16] T. Granier, B. Gallois, J. Gaultier, J. A. Real and J. Zarembowitch, *Inorg. Chem.*, 1993, **32**, 5305-5312.
- [17] V. Legrand, F. Le Gac, P. Guionneau and J. F. Letard, *J. Appl. Cryst.*, 2008, **41**, 637-640.

- [18] S. A. Moggach, T. D. Bennett and A. K. Cheetham, *Angew. Chem., Int. Ed.*, 2009, **48**, 7087-7089.
- [19] A. W.-H. Lam, W.-T. Wong, S. Gao, G. Wen and X.-X. Zhang, *Eur. J. Inorg. Chem.*, 2003, 149-163.
- [20] L. Merrill and W. A. Bassett, *Rev. Sci. Instr.*, 1974, **45**, 290-294.
- [21] S. A. Moggach, D. R. Allan, S. Parsons and J. E. Warren, *J. Appl. Cryst.*, 2008, **41**, 249-251
- [22] G. J. Piermarini, S. Block, J. D. Barnett and R. A. Forman, *J. Appl. Phys.*, 1975, **46**, 2774-2780.
- [23] Bruker-Nonius, *SAINT version 7, Program for integration of area detector data*, (2006).
- [24] G. M. Sheldrick, *SADABS Version 2008-1*, (2008) University of Göttingen, Göttingen, Germany.
- [25] P. W. Betteridge, J. R. Carruthers, R. I. Cooper, K. Prout and D. J. Watkin, *J. Appl. Cryst.*, 2003, **36**, 1487.
- [26] A. Dawson, D. R. Allan, S. Parsons and M. Ruf, *J. Appl. Cryst.*, 2004, **37**, 410-416.
- [27] A. Altomare, G. Cascarano, C. Giacovazzo and A. Guagliardi, *J. Appl. Cryst.*, 1993, **26**, 343-350.
- [28] CrystalImpact, *DIAMOND version 3.0, Visual crystal structure information system.*, (2004.) Crystal Impact GbR, Postfach 1251, 53002, Bonn, Germany.
- [29] G. M. Sheldrick, *SHELXTL-XP version 6.01*, (2001) University of Göttingen, Germany and Bruker-AXS, Göttingen, Germany and Madison, Wisconsin, USA.
- [30] C. F. Macrae, I. J. Bruno, J. A. Chisholm, P. R. Edgington, P. McCabe, E. Pidcock, L. Rodriguez-Monge, R. Taylor, J. van de Streek and P. A. Wood, *J. Appl. Cryst.*, 2008, **41**, 466-470
- [31] CrystalMaker, *A crystal and molecular structures program for MAC and Windows.*, (2009), Oxford, UK.
- [32] A. L. Spek, *J. Appl. Cryst.*, 2003, **36**, 7-13.
- [33] L. J. Farrugia, *J. Appl. Cryst.*, 1999, **32**, 837-838.
- [34] R. J. Angel, *Reviews in Mineralogy & Geochemistry*, 2001, **41**, 35-59.
- [35] R. J. Angel, *EOSFIT version 5.2*, (2002) Virginia Tech, Blacksburg, VA, USA.
- [36] R. J. Angel, *NATO Science Series, II: Mathematics, Physics and Chemistry*, 2004, **140**, 21-36.
- [37] G. R. Desiraju and T. Steiner, *The Weak Hydrogen Bond in Structural Chemistry and Biology*, Oxford University Press, Oxford, UK, 1999.
- [38] P. Vinet, J. H. Rose, J. Ferrante and J. R. Smith, *J. Phys.: Condens. Matter*, 1989, **1**, 1941-1963.

- [39] P. Vinet, J. R. Smith, J. Ferrante and J. H. Rose, *Phys. Rev. B: Condens. Matter*, 1987, **35**, 1945-1953.
- [40] N. P. Funnell, A. Dawson, D. Francis, A. R. Lennie, W. G. Marshall, S. A. Moggach, J. E. Warren and S. Parsons, *Submitted for publication*, 2010.
- [41] S. Jun-Ling and M. Jiang-Gao, *Chem. - Eur. J.*, 2005, **11**, 1417-1424.
- [42] P. A. Wood, J. J. McKinnon, S. Parsons, E. Pidcock and M. A. Spackman, *CrystEngComm*, 2008, **10**, 368-376.